



Design and Characterization of an Inhalation System to Expose Rodents to Nanoaerosols

Frédéric Cosnier, Sébastien Bau^{*}, Stéphane Grossmann, Hervé Nunge, Céline Brochard, Stéphane Viton, Raphaël Payet, Olivier Witschger, Laurent Gaté

Institut National de Recherche et de Sécurité, Rue du Morvan CS 60027, 54519 Vandoeuvre-lès-Nancy, France

ABSTRACT

The number of workers potentially exposed to nanoparticles (NPs) in industrial processes is constantly increasing, even though the toxicological effects of these compounds have not yet been fully characterized. The hazards associated with this exposure can be assessed most relevantly by toxicology studies involving inhalation of nanoaerosols by animals.

In this paper, we describe and characterize an aerosol generated in a nose-only exposure system used to study the respiratory effects of NPs in rat; this system was designed to meet the most stringent requirements for animal testing in terms of protection of operators against risks associated with NPs and biohazards and to comply with the OECD guidelines for chemical testing.

The inhalation facility was fully validated by exposing Fisher 344 rats to TiO₂ P25 aerosols at 10 mg m⁻³. Aerosol monitoring and in-depth characterization were ensured by real-time devices (condensation particle counter, optical particle sizer, scanning mobility particle sizer, aerodynamic particle sizer and electrical low pressure impactor) and samples taken for off-line analyses (gravimetric analysis, mass size distribution from cascade impactor, TEM observations).

The test atmosphere was stable in terms of concentrations and distributions (mass or number) between different inhalation towers on a given day and between days (intra-experiment), as well as between inhalation campaigns (between experiments). In terms of the respiratory deposition profile, preliminary results after exposure for one month indicate that this system is relevant, and should therefore be appropriate for in vivo inhalation toxicity studies.

Keywords: Inhalation; Rodent; Nanoaerosols; Titanium dioxide.

INTRODUCTION

Due to the growing use of nanoparticles (NPs) in industrial processes, the number of workers potentially exposed to these compounds is increasing even though their toxicological effects have not yet been fully characterized. Because inhalation represents the main route of occupational exposure to airborne nanoparticles, the first line of exposure is the respiratory system. For this reason, toxicology studies involving inhalation of nanoaerosols by animals appear to be the most relevant to assess the hazards associated with exposure to these particles.

Besides, there is an important need for harmonizing the procedures for aerosol characterization in inhalation toxicological studies. To obtain relevant inhalation toxicity data and ensure inter-experiment comparability, it is crucial that the nanoaerosol generation methods and physico-

chemical characterization approaches reflect conditions in industry. For in vivo inhalation toxicity studies, it remains challenging to generate stable, reproducible aerosols for several hours per day, over several days or weeks.

Two different approaches are generally considered in experimental inhalation studies; the first corresponds to the “direct synthesis method” which uses a non-particulate substrate as a source of nanoparticles, the second involves wet or dry systems generating nanoaerosols from nanostructured powders (Morimoto *et al.*, 2013). Since more than half of the industrial activities using nanopowders involve mixing (for the formulation of preparation) and transfer (loading, unloading, weighing) operations, dry generation methods appear better reflect industrial conditions (MDDE, 2014).

Various systems to test inhalation toxicity based on dry generation from powders have been described, among which the acoustic generator (McKinney *et al.*, 2009), the fluidized bed aerosol generator (Nurkiewicz *et al.*, 2008; Noel *et al.*, 2013), the jet mill (Mitchell *et al.*, 2007), the rotating brush generator (RBG) (Bermudez *et al.*, 2004; Ma-Hock *et al.*, 2009), the Wright dust feeder (Pauluhn, 2010) and the low-cost powder disperser (Tiwari *et al.*, 2013).

According to the 2014 summary document derived from

^{*} Corresponding author.

Tel.: (+33) (0)3 83 50 98 90; Fax: (+33) (0)3 83 50 87 11
E-mail address: sebastien.bau@inrs.fr

the compulsory French “Nanomaterials” registry (MDDE, 2014), in France the most frequently produced or imported nanomaterials are carbon black (and related compounds), SiO₂, CaCO₃, TiO₂ and Al₂O₃. Although it might be relevant to test all of these materials, it could be useful to determine a “reference” nanoparticle, as has been done for fibers (UICC asbestos) and micrometric particles (quartz DQ12). Currently, one of the most studied nanoparticles *in vitro* and *in vivo* is TiO₂ P25 Evonik (OECD, 2015). This compound is also a NIST Standard Reference Material, and thus represents a potential candidate as a reference toxicological nanoparticle. P25 is a mixed-phase nanocrystalline dry powder composed of 75% anatase and 25% rutile crystallites, with an average primary particle diameter of 25 nm. TiO₂ is widely used as a photocatalyst, a sterilizing agent and an ultraviolet blocker.

This paper describes a system for aerosol generation and inhalation allowing the study of the respiratory effects of NPs in rat and its characterization. The system, called *NanoTIREx* (for Nanomaterial Toxicology Inhalation system for Rodent Exposure), was designed to meet the most stringent requirements for animal testing in terms of protection of operators against risks associated with NPs and biohazards, and to comply with the OECD guidelines for chemical testing (TG412 and TG413). The system has been fully validated through exposure of Fisher 344 rats to TiO₂ P25 aerosols at a target concentration of 10 mg m⁻³.

MATERIALS AND METHODS

Description of the Experimental Facility for Rodent Exposure

The experimental set up (Fig. 1) consists of an aerosol generation system and inhalation towers for nose-only exposure (EMMS, Electro-Medical Measurement System, Bordon, UK).

Towers are made from stainless steel and anodized aluminum to minimize electrostatic losses and reduce the possibility of contamination. Two types of towers were used: single level tower (9-port) for rats exposed to airborne nanomaterials (Fig. 2(a)) and 3-level tower (3 × 9-port) for control rats; both have a by-pass flow (double plenum) designed to avoid mixing of inlet and exhaust flows (the one exhaled by the animals and the excess aerosol flow). Each exposure port has its own separated channel within the double plenum. The aerosol is directed to the exposure ports by means of a flow splitting cone from the central cylinder (Fig. 2(b)). Finally, rats held in restraining tubes attached to the towers are nose-only exposed to the aerosol. The total exposure capability is over 100 rats: 50 nanomaterials - exposed rats (exposed through 6 × 9-port tower) and 50 control rats (through 2 × 27-port tower).

Aerosol generation was performed in a different room to inhalation exposure. Aerosols were produced by a rotating brush (RBG1000, reservoir diameter 7 mm, Palas, Karlsruhe, Germany), placed under a laminar flow fume hood. Dry, filtered compressed air (Donaldson Ultrafilter 4812) was used as the carrier gas. This generation system was chosen because it can deliver a relatively high, stable mass concentration of TiO₂ aerosol for several hours (Bermudez

et al., 2004; Ma-Hock *et al.*, 2009; Noel *et al.*, 2013). In line with OECD guidelines (OECD, 2009), the aerosol was conditioned at 22 ± 2°C and relative humidity (RH) 55 ± 10% by diluting it with air which had passed through a packed-tower humidifier. The diluted aerosol transited through stainless steel and antistatic perfluoroalkoxy tubing to reach the inhalation towers. In parallel, control rats were exposed to (particle-free) filtered air only (SMC IDG10-F03) (same air quality than that used for exposed rats) also conditioned at 22 ± 2°C and RH 55 ± 10%. Airflows (5 L min⁻¹ for exposure towers and 15 L min⁻¹ for control towers) were pump-aspirated at the outlet of the towers to create a slight negative pressure (−1.5 mbar). Both exposure towers and control towers were placed in containment boxes.

The integrated control of the exposure conditions (flow rates, temperature, RH, relative pressure, etc.) was managed and recorded using dedicated software.

Aerosol monitoring and characterization were performed directly on the inhalation towers (Fig. 2(a)) using a sampling probe fitting the conical portion of the restraining tubes (Fig. 2(c)) which was placed on one of the 9 ports of the tower (Fig. 2(d)).

Animal Exposure

Animal experiments were performed in line with European and French regulations relating to the protection of animals used for scientific purposes (European Directive 2010/63/EU) in a French Ministry of Agriculture-accredited animal facility (Accreditation N° D54-547-10). Protocols were approved by the local Ethics Committee (C2EA-66: Comité d'éthique Lorrain en Matière d'Expérimentation Animale) and the French Ministry for Research and Higher Education (authorization No. 00692.01).

13-week-old male Fisher F344 rats (Charles River Laboratories, France) weighing between 310 and 360 g were used in this study. Animals were housed in standard environmental conditions (RH 55 ± 10% and temperature maintained at 22 ± 2°C; 12/12 h light/dark cycle). Water and a standard laboratory diet (A04 Safe diet) were freely available. One week before the beginning of the exposure period, rats were gradually acclimatized to the restraining tubes and conditions required for the experiment: 2 periods of 3 h exposure.

Rats were then exposed to either fresh air (control group; $n = 2 \times 24$) or TiO₂ NP aerosols at 10 mg m⁻³ (treated group; $n = 4 \times 8$) for 2 periods of 3 h per day, 5 days/week for 4 weeks. The animals were rotated daily between the various towers daily to avoid tower-related variations.

After the end of the inhalation exposure period, 6 animals were anesthetized with pentobarbital (60 mg kg⁻¹) and exsanguinated through the abdominal aorta. Lungs and other tissues were collected and stored at −80°C prior to analysis. The Ti burden in the lungs was analyzed by ICP-MS, as previously described (Devoy *et al.*, 2016).

Aerosol Monitoring during Inhalation

An optical particle counter (OPC FIDAS mobile, Palas, $Q_{\text{aerosol}} = 1.4 \text{ L min}^{-1}$) was used to monitor the aerosol characteristics in real-time, the generation process could

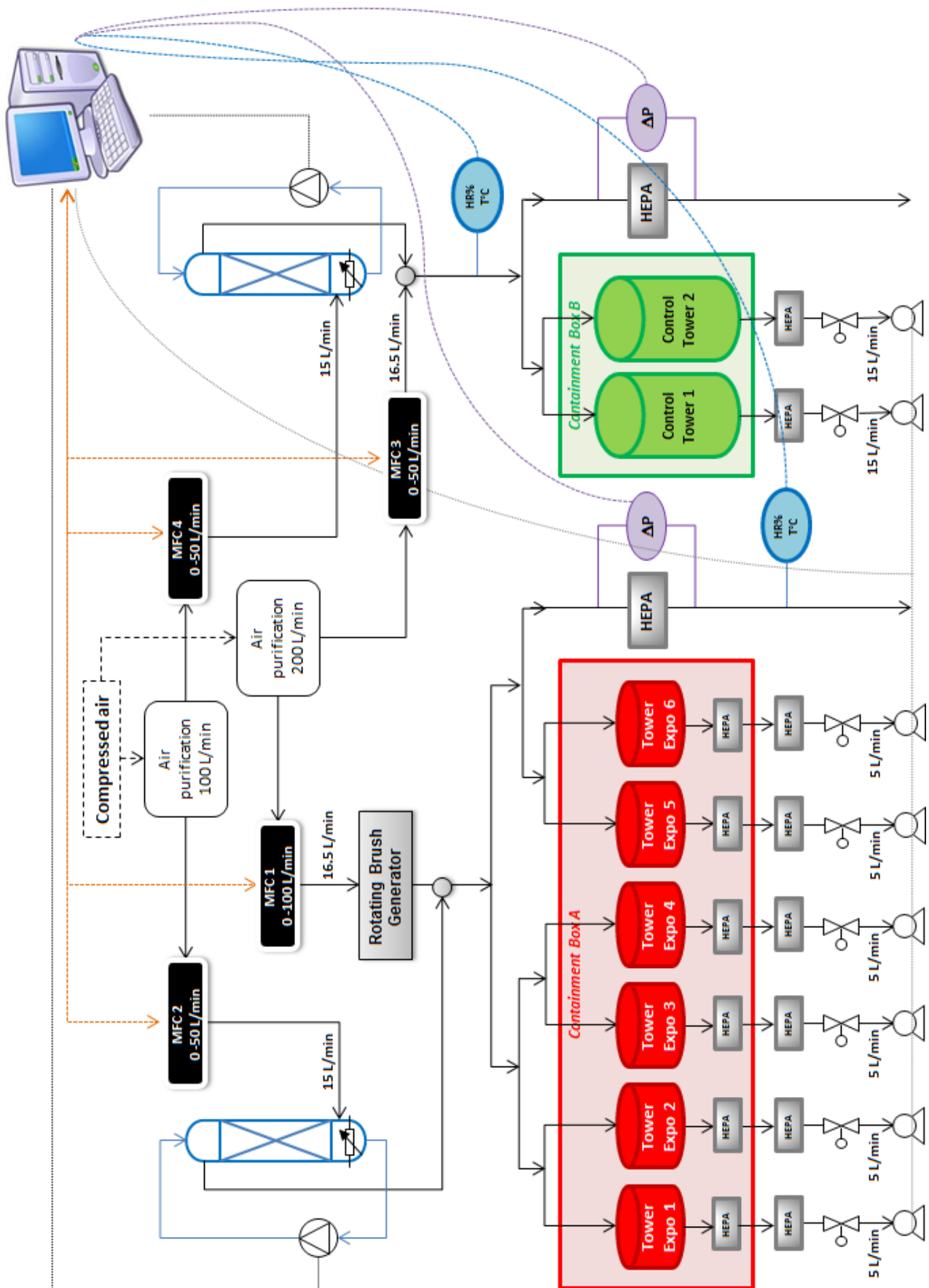


Fig. 1. Description of the NanoTTREX experimental set up.

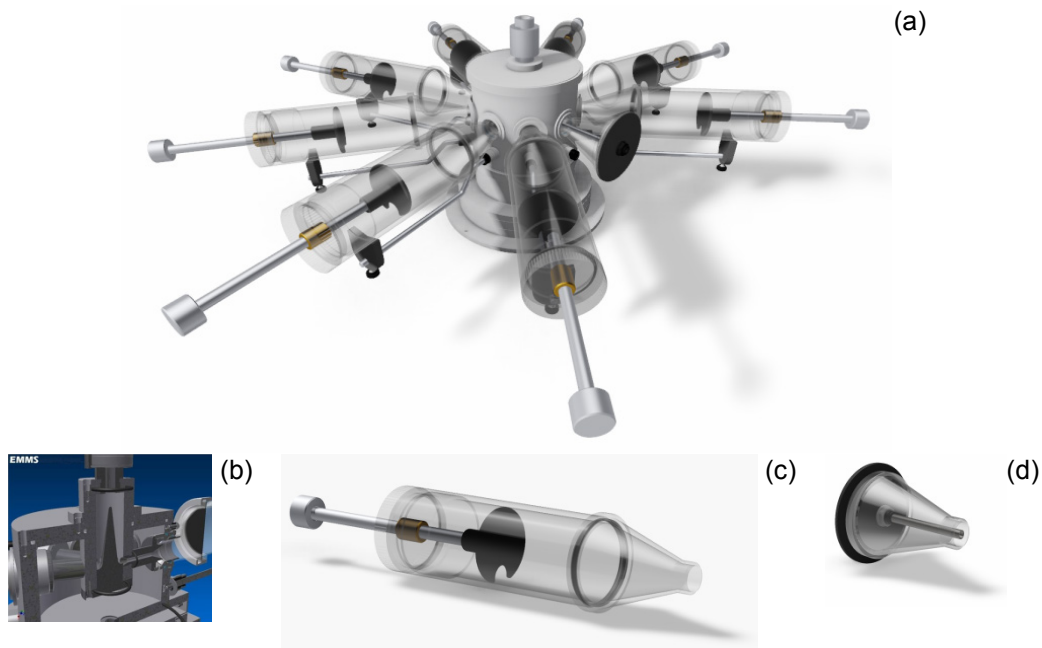


Fig. 2. Single level inhalation tower (EMMS, Bordon, UK) (a) with cross-sectionnal view (b), 8 home-made contention tubes (c) and one sampling probe (d).

thus be adapted if necessary. This device measures total particle number concentration and particle number size distribution (0.18–18 μm) in real-time (1 Hz). Because of limited sampling possibilities, the aerosol was diluted roughly 15-fold by adding an appropriate and controlled (Brooks 5051S) HEPA-filtered air flow.

This OPC can also measure mass concentration by performing calculations using the number size distribution measured and making some assumptions relating to particle density (standard or user-defined constant density) and shape (spherical particles). Although the device can be calibrated to improve accuracy, it was not deemed necessary for this work, and only the particle number size distribution was considered as a monitoring parameter. The refractive index of airborne particles was taken as equal to 1.

To determine the mass concentration, aerosols were sampled using a 25-mm closed-face cassette (Merck-Millipore) containing PVC membrane filters (GLA-5000, 5 μm pore size). Gravimetric measurements were performed using a microbalance (Mettler XP6U, 0.1 μg resolution) placed in a dedicated room where temperature ($22 \pm 2^\circ\text{C}$) and RH ($50 \pm 10\%$) were controlled. A personal air sampling pump (Gilian 5000, Sensidyne) operating at a flow rate of 1 L min^{-1} (preliminarily calibrated, controlled before and after sampling with a calibrated TSI mass flowmeter model 4043) was used to sample aerosols in the cassette. Samples were taken twice (or four times) daily for approximately 90 minutes (about 0.9 mg collected on filters).

Airborne particle mass size distribution was measured using a cascade impactor (SIOUTAS PCIS, SKC, $Q_{\text{aerosol}} = 9 \text{ L min}^{-1}$). The impaction plates were equipped with 25-mm membranes (PVC, GLA-5000, 5 μm pores), and the terminal filter was a 37-mm PTFE membrane with PMP support ring (SKC, 2 μm pores). The membranes placed on the impaction

stages were not greased prior to aerosol sampling, as suggested in the user manual. A personal air sampling pump (GSA, SG10-2) (controlled before and after sampling) was chosen to maintain a constant flow rate despite the quite large pressure drop. Samples were taken twice weekly for approximately 90 minutes. All filters were weighed using the microbalance described above.

The raw data (mass size distribution) were further transformed by an inversion procedure, as detailed in Bau and Witschger (2013), based on the collection efficiencies of the impaction stages reported by Misra *et al.* (2002). This method takes into account the existing overlap between the successive impaction stages, i.e., particles of a given diameter can be deposited on several stages due to steep collection efficiency curves and particle bounce (Dong *et al.*, 2004). The inversion procedure is based on a deterministic method first described by Twomey (1975), and subsequently improved by various authors (Markowski, 1987; Winklmayr *et al.*, 1990). Among its main advantages, this nonlinear iterative method does not assume any mathematical model for the resulting aerosol size distribution. The size distribution can therefore be smoothed to make it more physically relevant. In this study, the discrepancy tolerated between the mass concentrations measured and those calculated from the inverted curve was set to $1/10^{\text{th}}$ of the smallest concentration.

Aerosol Characterization

The aerosols were characterized in detail by taking various measurements covering a wide range of particle sizes and properties. In particular, particle number size distribution was measured in the sub micrometer range (10 nm to 1000 nm) using a scanning mobility particle sizer (SMPS+C, Grimm, composed of a Vienna-type Differential Mobility Analyzer and a Condensation Particle Counter

(CPC) 5.403; $Q_{\text{aerosol}} = 0.3 \text{ L min}^{-1}$, $Q_{\text{sheath}} = 3 \text{ L min}^{-1}$, $d_{50} = 4.5 \text{ nm}$). Data in the micrometer range (0.52 μm to 20 μm) were acquired with an aerodynamic particle sizer (TSI APS model 3321; $Q_{\text{aerosol}} = 5 \text{ L min}^{-1}$).

In addition, particle mass size distribution over a wide range of sizes, from 0.03 μm to 10 μm , was obtained with an electrical low pressure impactor (ELPI, Dekati, $Q_{\text{aerosol}} = 10 \text{ L min}^{-1}$). This mass size distribution was inverted by applying the procedure described above (Bau and Witschger, 2013) and the collection efficiency curves described in Marjamäki *et al.* (2005).

Finally, the electrical state-of-charge for particles was determined by combining airborne particle current and number size distributions measured by an ELPI, as detailed in Simon *et al.* (2015). With this method, the net number of elementary electrical charges $p(d_a)$ carried per particle was determined in each channel by applying the following formula (Eq. (1)):

$$p(d_a) = \frac{I(d_a)}{C_N(d_a)eQ} \quad (1)$$

where I is the current, d_a is the particle aerodynamic diameter, C_N is the number concentration, e is the elementary charge, and Q is the volumetric flow rate.

Estimated Fraction Deposited in the Respiratory Tract

The fraction deposited in the respiratory tract was estimated using the deposition module of the Multiple-Path Particle Dosimetry Model (MPPD V2.11) (<http://www.ara.com/products/mppd.htm>). The airway morphometry and respiratory parameters for F344 rats used as input data were those determined by Hsieh *et al.* (1999), and Menache *et al.* (1997). Thus, functional residual capacity, upper respiratory tract, tidal volume and breathing frequency were set to 2.1 mL, 0.5 mL, 1.9 mL and 120 per min, respectively.

EXPERIMENTAL RESULTS

Primary Qualification

Prior to each aerosol generation, the facility was tested with HEPA-filtered air to monitor for leaks within the setup, and a zero concentration was measured using the CPC.

Preliminary experiments verified the homogeneity of the aerosol concentration between the different inhalation towers; the homogeneity within a given tower was ensured by the symmetry of its internal geometry. These verifications were performed using particles produced by atomization (TSI 3076 Constant Output Atomizer) of an aqueous solution (NaCl 1 g L⁻¹); which resulted in airborne particles with a count median diameter below 50 nm. A first CPC (TSI, model 3007) was placed directly at the outlet of the atomizer, while a second CPC sampled aerosols in each of the 6 inhalation towers successively. The number concentrations measured in the inhalation towers were compared to those simultaneously measured at the generator outlet.

The average ratio measured was 0.79 ± 0.03 , for all the inhalation towers. The variability in ratio between the

different ports of a given tower was found below 3.5%. Taken altogether, the overall variability in the concentration ratio between all ports was found to be 3.7%. This confirms the homogeneity of the aerosol delivered and of the system as a whole. These data are in line with the ones recently published by Buckley *et al.* (2016), who describe the inhalation of radioactive iridium-192 nanoparticle aerosol in a similar inhalation facility.

Aerosol Monitoring

Number Concentration

A typical profile of how the number concentration changes over time during exposure to airborne TiO₂ particles is presented in Fig. 3(a). The daily variation coefficient of the number concentration never exceeded 15%. This profile was obtained from the raw data corrected for the dilution factor. Dilution was useful to avoid measurement problems, by maintaining particle coincidence within the OPC at less than 10%. By adjusting the feed rate of the RBG operated at constant air flow, an aerosol could be stably generated over six hours. In practice, the reservoir had to be filled twice a day with about 800 mg of dry powder; the powder bed was then pre-compacted before introducing it into the generator. Due to the high abrasiveness of TiO₂ P25 powder, the standard piston seal had to be replaced by a homemade Teflon seal. Number concentration profiles were measured with a CPC (TSI, model 3007, data not shown), with similar profiles obtained throughout the generation period and with each batch of powder. The average number concentration during the six 20-day campaigns of exposure was 24,000 particles cm⁻³ (± 6400 Standard Deviation) (diameter > 10 nm).

As shown in Fig. 3(b) (for a single day's exposure), stability of the relative number size distribution was also verified during the exposure periods for aerosols with a modal diameter around 300 nm.

Mass Concentration

Six inhalation campaigns have been performed so far, and the statistics in terms of mass concentration are summarized in Table 1. The actual mean mass concentrations of the six exposure campaigns were close to the target concentration (10 mg m⁻³) and any difference between the six mass concentration averages were not statistically significant based on the 95% confidence interval. For the first four exposures, the coefficients of variation were greater than 20%, which is the limit recommended by the OECD test guideline 412 "Subacute Inhalation Toxicity: 28-Day Study" for inhalation exposure to liquid or solid aerosols. This coefficient of variation was limited to 14% when a photometer (Thermo Scientific pDR-1500 personal DataRAM) was implemented on the inhalation tower to monitor the mass concentration (Exposure campaigns 5 and 6).

Aerosol Characterization

Number Size Distribution

The number size distribution of airborne particles is presented in Fig. 4, with error bars representing the 95% confidence interval. To merge the two data series, which

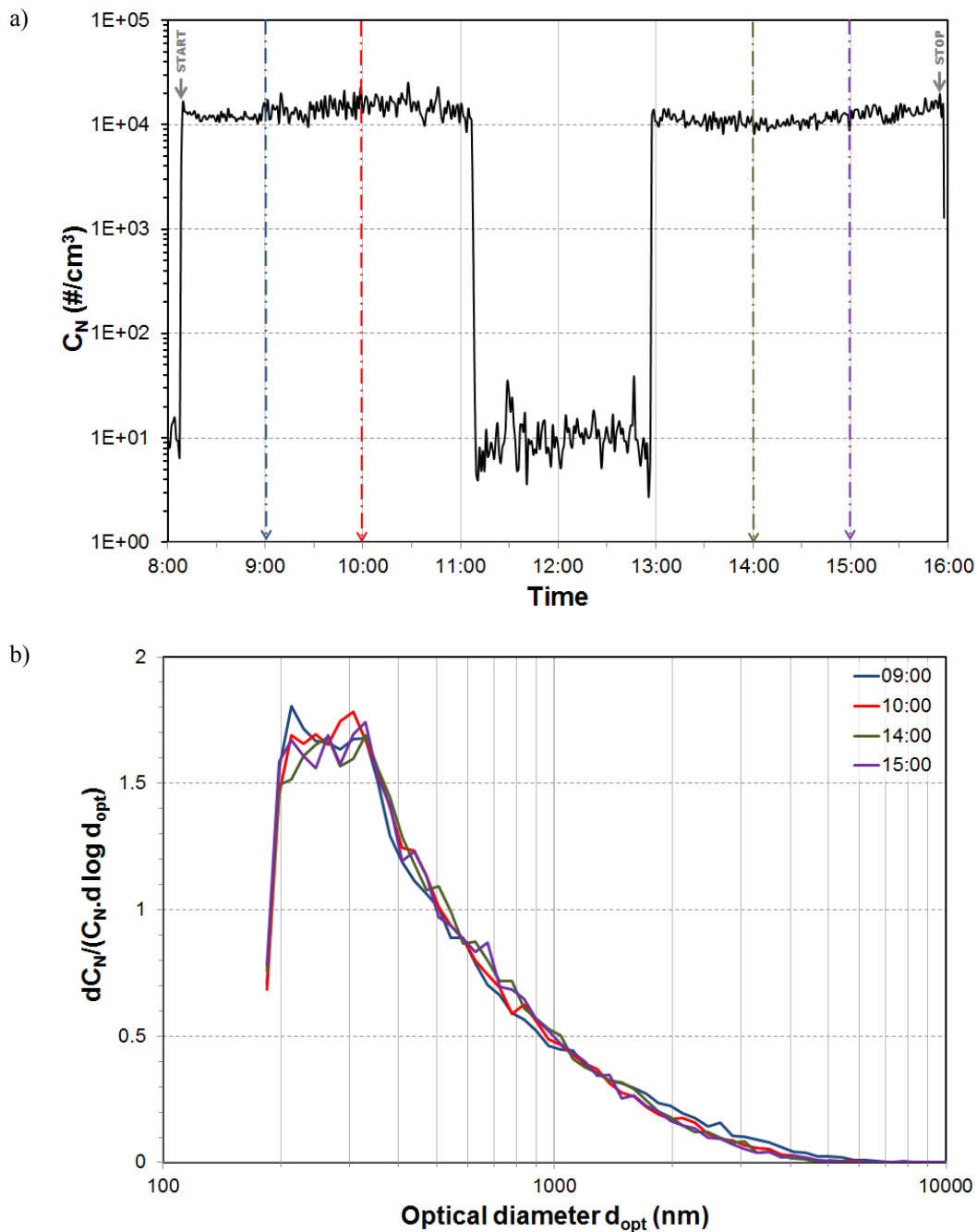


Fig 3. Number concentration profile over time during animal exposure, as observed with FIDAS Mobile (a) and relative number size distributions at four different times (b) (Data exported from PDAAnalyse Software Ver. 2.024).

Table 1. Mass concentration statistics of the six inhalation campaigns.

Exposure campaign	Mean concentration [#] (mg m ⁻³)	Standard deviation	Coefficient of variation (%)	Median	Minimum	Maximum
1	9.91	3.35	33.8	8.75	4.58	21.29
2	9.85	2.78	28.3	9.71	4.01	16.57
3	10.60	3.07	28.9	10.36	5.04	17.30
4	10.74	2.48	23.1	10.48	6.06	17.12
5	10.25	1.39	13.6	10.16	8.14	13.86
6	10.27	1.25	12.1	10.07	8.23	13.25

[#] Gravimetric measurements were performed twice and four times a day for exposure campaigns 1 to 3 and 4 to 6, respectively.

involve two different concepts of particle equivalent diameter, the aerodynamic diameters measured by the APS were converted into mobility equivalent diameters using the formula (Eq. (2)) proposed by De Carlo *et al.* (2004), where d_a and d_m are the equivalent aerodynamic and electrical mobility diameters, Cu the slip correction factor in molecular and transition regimes, ρ_p particle density and $\rho_0 = 1 \text{ g cm}^{-3}$ the standard density.

$$d_a = d_m \left(\frac{Cu(d_m) \rho_p}{Cu(d_a) \rho_0} \right)^{1/2} \quad (2)$$

Thus, particle density was adjusted to cause both number size distributions to overlap in the range of sizes from roughly 0.7 μm to 1.1 μm . A particle density of 620 kg m^{-3} was determined based on this data treatment. In spite of its theoretical size-dependence (Virtanen *et al.*, 2004; Charvet *et al.*, 2014), this density value was considered to be constant for the remainder of this paper. To rigorously determine particle effective density with regards to particle diameter would involve a more complex experimental setup, which we considered beyond the needs of this study.

As shown in Fig. 4, the number size distribution was monomodal, with particles ranging in diameter roughly from 40 nm to 3 μm . Experimental data were fitted by a lognormal model according to the Least Squares Method, the Count Median Mobility Diameter (CMMD) determined was 347 nm, with a Geometric Standard Deviation (GSD) of 2.29. Expressed in terms of aerodynamic diameters, this resulted in a Count Median Aerodynamic Diameter (CMAD) of 269 nm, with a GSD of 2.22.

Mass Size Distribution

The “routine” use of the cascade impactor allowed robust characterization of the airborne particles mass size

distribution (Fig. 5). The data presented in this figure represent the mean from 24 measurements.

Fig. 5 also presents ELPI data, calculated from the current size distribution measured and converted into a mass distribution based on the particle density mentioned above (620 kg m^{-3}) and assuming spherical particles (Eq. (3)):

$$C_M(d_p) = C_N(d_p) \frac{\pi}{6} d_p^3 \rho_p \quad (3)$$

where $C_M(d_p)$ and $C_N(d_p)$ are the mass and number concentrations of particles with diameter d_p . It should be noted that this assumed constant density, even though it does not entirely reflect the truth, provides a satisfactory indication of the airborne particle mass concentration. However, this assumption could lead to large discrepancies if used to calculate a number size distribution or concentration (Charvet *et al.*, 2016).

Fig. 5 shows an acceptable correlation between SIOUTAS and ELPI-based mass size distributions (bias $\approx 44\%$ on the modal diameter). More precisely, the mass modal aerodynamic diameters calculated were 1.18 μm for SIOUTAS data and 1.70 μm for ELPI data.

The mass size distribution measured by gravimetric analysis in the SIOUTAS cascade impactor revealed that almost 80% of the total mass of airborne particles corresponded to particles with diameters from 250 nm to 2500 nm. According to our results, these three impaction stages contribute to the total mass roughly to the same extent (29% for stage 250–500 nm, 28% for stage 500–1000 nm, and 34% for stage 1000–2500 nm). Based on the cumulative mass distribution, the mass median aerodynamic diameter (MMAD) was determined to be 0.905 μm , with a GSD of 2.19.

ELPI-based mass size distribution was somewhat different, suggesting (1) an almost total absence of particles below

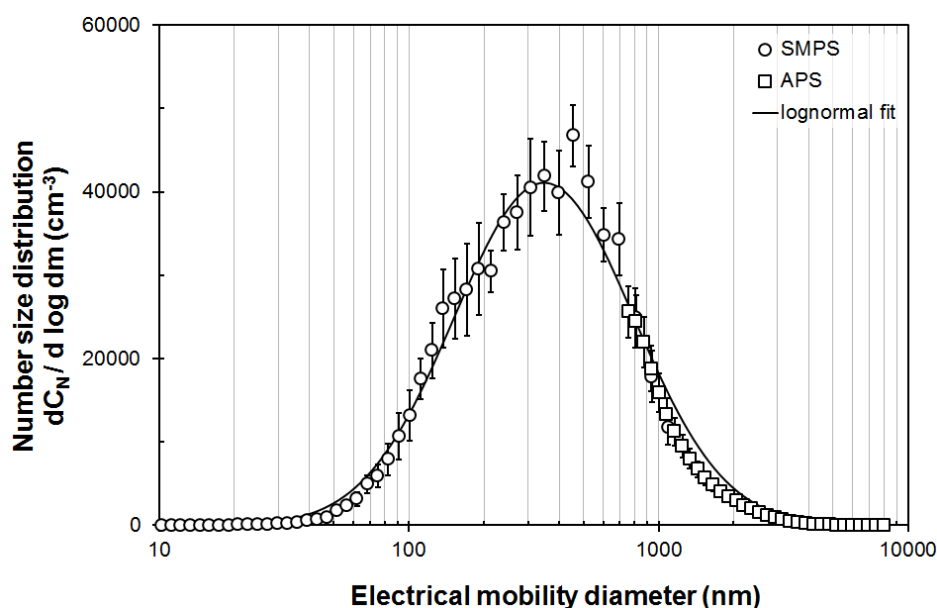


Fig. 4. Airborne particle number size distribution as measured by SMPS and APS.

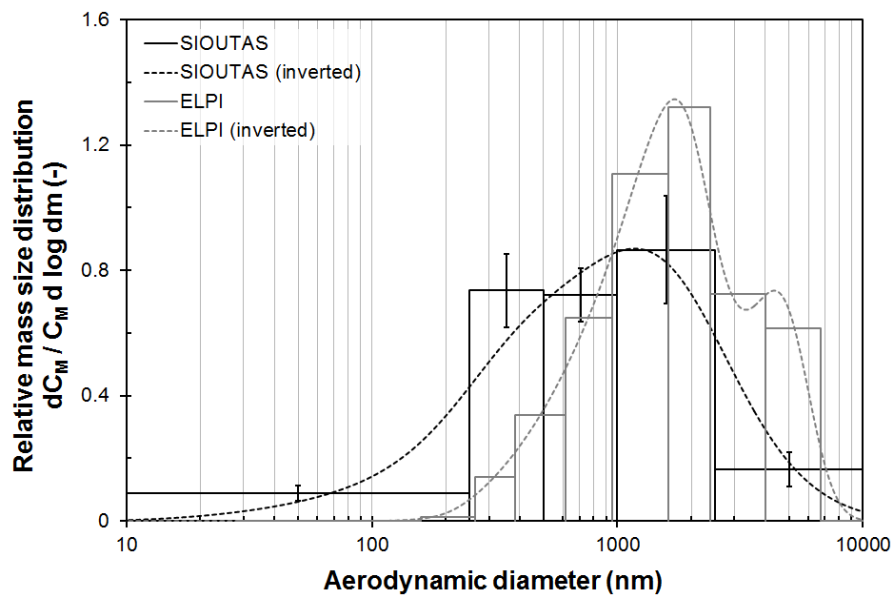


Fig. 5. Airborne particle relative mass size distribution and inversion curves based on cascade impactor data (SIOUTAS & ELPI).

200 nm, and (2) presence of a second mode, between 4 and 5 μm . With regard to this second mode, it is important to point out that any current measured on an impaction stage will result in a significant overestimation of the mass concentration (Maricq *et al.*, 2006; Zervas *et al.*, 2006).

The number size distribution from both SMPS and APS was also converted into mass size distribution using the same formula (data not shown). These distributions were found to be monomodal, with a mass modal aerodynamic diameter of 1.72 μm (MMAD = 1.65 μm), which is in line with the results mentioned above.

The slight shift in the mass size distribution towards lower particle sizes with the SIOUTAS impactor may be due to particle bouncing as we chose not to grease the impaction plates.

Net Number of Elementary Electrical Charges per Particle

Several processes contribute to the charging of aerosol particles. For the particular case of aerosols produced from powders, the main mechanisms of charge transfer involve particles striking each other and/or bouncing off other structures. A particle's electrical state-of-charge can affect its deposition in the lung, its collection efficiency on filters, its transport (e.g., deposition in sampling lines) and its behavior during sampling processes. Thus, it is important to determine the overall electrical charge carried by airborne particles.

Measurements were performed with the ELPI with and without a charger and ion trap to determine the average net number of electrical charges carried by particles. Because charging mechanisms are related to the electrical properties of particles, the data were expressed as an electrical mobility equivalent diameter (Fig. 6). The results indicate a negative state-of-charge; the number of elementary charges varies from -4.3 [e] for 400-nm particles to -390 [e] for 6600-nm particles. In addition, the curve describing $p(d_m)$ is well fitted ($R^2 = 0.983$) by a power law, with an exponent of 1.57. This

experimental curve fitting suggests that the surface area of airborne particles also affects charging mechanisms.

Electron Microscopy

The aerosol was directly collected on transmission electron microscopy grids (using a mini particle sampler, MPS ECOMESURE) to characterize particle morphology (R'Mili *et al.*, 2013). The photos presented in Fig. 7 show that the particles (primary size of about 25 nm) are in the form of agglomerates measuring several hundred nanometers to a few micrometers. These observations are consistent with the results of aerosol measurement. The agglomerates mainly consisted of the anatase crystallographic form of TiO_2 , in agreement with observations of the powder from which the aerosol was generated (Ohtani *et al.*, 2010; Disdier *et al.*, 2015).

Respiratory Tract Deposition

After exposure for 1 month, ICPMS measurements detected 2086 ± 94 μg (mean \pm SD) of titanium in rat lungs ($n = 6$). Assuming that the rats have a respiratory minute volume of 228 mL min^{-1} (= tidal volume \times breathing frequency = 1.9×120), this corresponds to a deposited fraction of 0.212.

The airway deposited fraction was estimated by using the Multiple-Path Particle Dosimetry Model for rat based on (1) an aerosol with a MMAD of 905 nm and a GSD of 2.19 as stemming from SIOUTAS analyses, (2) a particle density of 4.23, corresponding to the one of the raw material required in the model rather than the effective density of airborne particles, and (3) an inspiratory fraction of 0.5 (default value). The deposited fraction (conduction airways + alveolar region) was found to be 0.129, which was close to the calculated fraction ($\sim 39\%$).

Indeed, in light of the uncertainty as to the physiological respiratory values for rats specified in the model, this

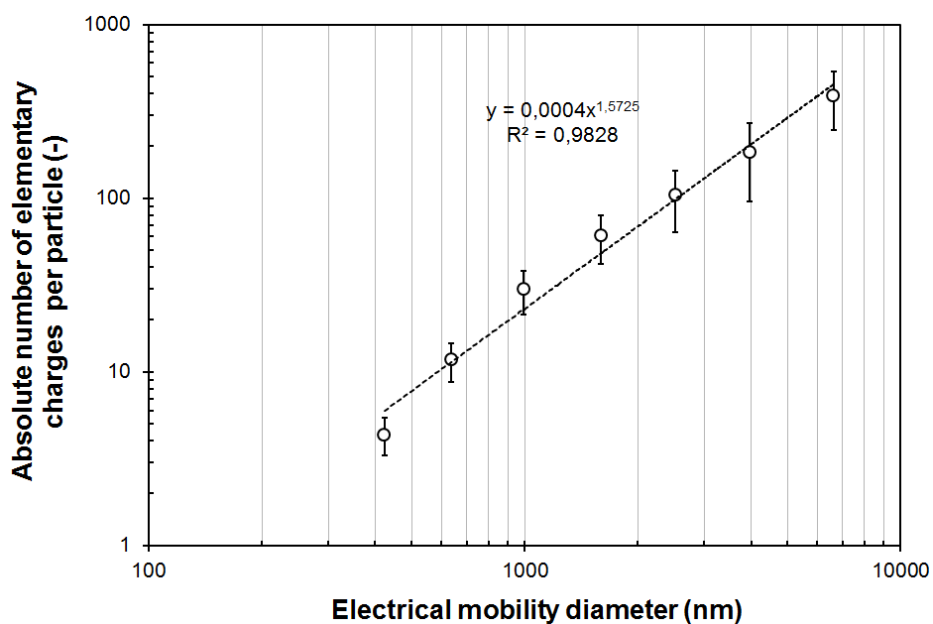


Fig. 6. Airborne particle absolute number of electrical elementary charges as a function of their mobility diameter. The error bars represent the 95% confidence interval.

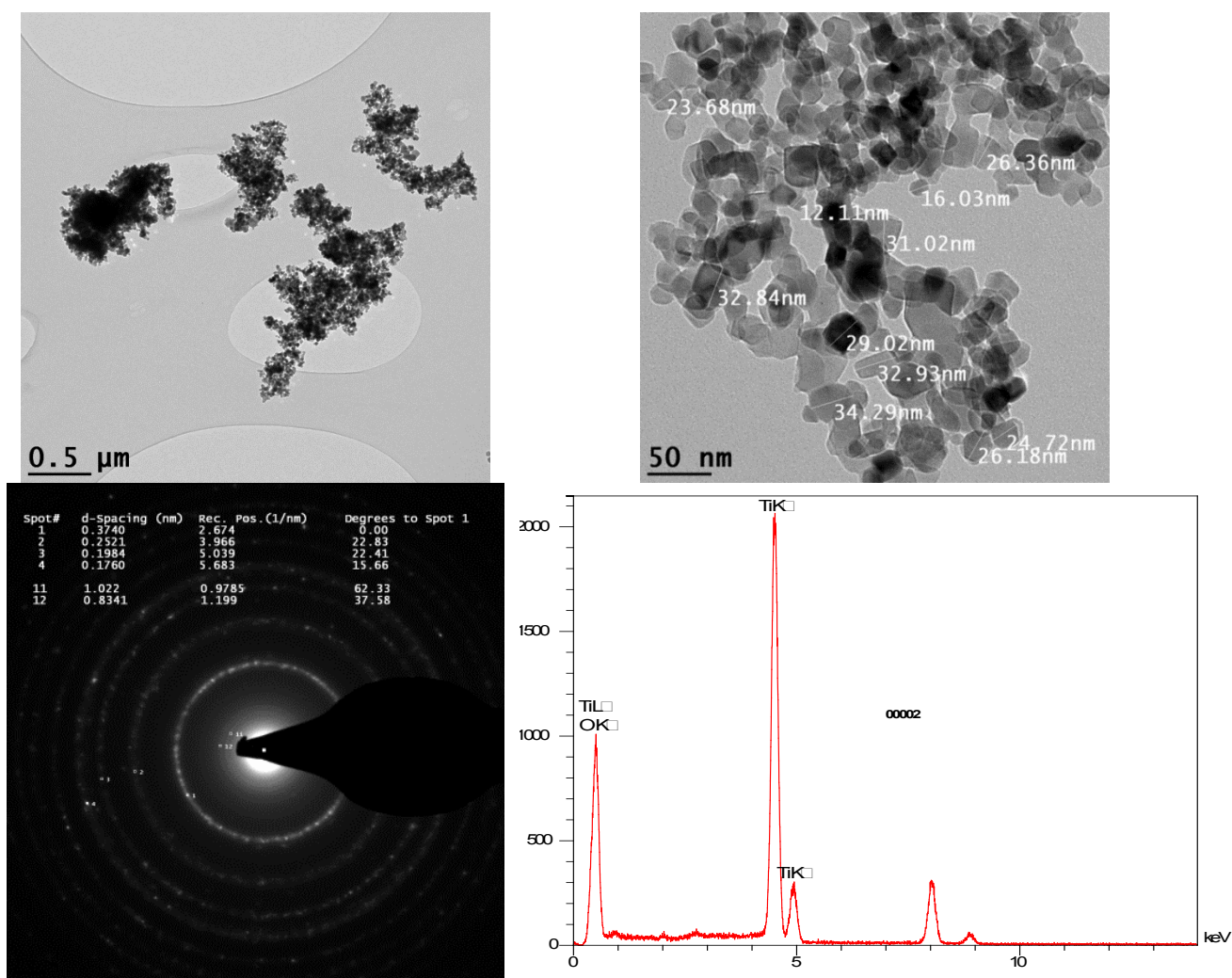


Fig. 7. TEM images and energy dispersive X-ray spectrum of a TiO_2 aerosol sample.

discrepancy is satisfying. For instance, if we considered the tidal volume determined by Mauderly (1982) for 3-month-old F344 rats (2.3 mL), the deposited fraction calculated would decrease to 0.175 (with a respiratory minute volume of 276 mL min⁻¹), whereas the deposited fraction estimated remained unchanged (0.130). This corresponds to a difference of 26%. In addition, the use of another MMAD (1.18 µm), obtained by inverting SIOUTAS data, can lead to an even lower estimation of the airway deposition fraction of 0.102.

DISCUSSION AND CONCLUSIONS

The results presented in this paper demonstrate that our safe experimental set up can generate a nanoaerosol suitable for *in vivo* subacute inhalation toxicity studies in rats.

Particular attention was paid to respecting of the criteria mentioned in the OECD inhalation guidelines TG412 and TG413 for chemical testing. Thus, the air flow through the exposure towers, maintained at 22 ± 2°C and a RH of 55 ± 10%, was carefully controlled, continuously monitored and recorded. This air flow is compatible with the respiratory physiology of rats (5 L per minute for each tower ≈ twice the respiratory volume per minute needed for nine restrained rats); in addition, the internal design of the inhalation towers prevented rebreathing.

In terms of concentrations (mass or number), the test atmosphere was demonstrated to be stable between inhalation towers on a given day, between days (intra-experiment) and also between inhalation campaigns (between experiments). According to OECD recommendation, individual samples to assess concentrations should deviate from the mean concentration by no more than 20% for liquid or solid aerosols. In our case, mean intra-experiment precision calculated from mass concentration data over the six inhalation campaigns was equal to 22%; when we only considered experiments monitored with an additional photometer this value was less than 14%. Moreover, reproducibility between experiments was proven by a variation coefficient of the average mass concentration of only 3.4%.

The aerosol of airborne TiO₂ produced was fully characterized in terms of number and mass size distribution and was found to be monomodal with a CMAD around 270 nm and an MMAD between 0.9 and 1.7 µm, the GSD for the distributions was 2.2–2.3. The primary particle size was small (25 nm), but the particles were mainly present in the test atmospheres in the form of agglomerates, in line with observations from Ma-Hock *et al.* (2009) and Bermudez *et al.* (2004) who generated aerosols of TiO₂ P25 in similar conditions (with rotating brushes). These test conditions are considered to be relevant, as they represent the exposure scenario occurring during occupational handling and processing of powder (Curwin and Bertke, 2011; Yang *et al.*, 2012).

Preliminary results obtained in rats exposed for 20 days demonstrated the relevance of our exposure system in terms of respiratory deposition, with a deposited fraction measured at 0.175; indeed, at the end of the exposure period, around 2 mg TiO₂ was determined per lung (or 1.4 mg g⁻¹ of lung).

Analysis of other inhalation experiments assessing the lung deposition of TiO₂ aerosols (target dose of 10 mg m⁻³), showed that the amount deposited in the conditions described here was 2.4-fold lower (after correction for exposure time) than the amount measured by Bermudez *et al.* (2004) after 13 weeks (65 days) (11 mg g⁻¹ of lung); however, it was equivalent to that measured by Ma-Hock *et al.* (2009) after 5 days (545 µg lung⁻¹). It should be noted that the calculated deposited fraction as well as the one estimated from the MPPD model are highly dependent of breathing parameters used. Since we were not able to measure these parameters under realistic conditions, we chose to use values stemming from previous work dedicated to their determination. As a consequence, the relative discrepancies between calculated and estimated fractions could be partly explained by the uncertainties on the set of parameters retained. In line with our observations, this point has been particularly addressed by Buckley *et al.* (2016), who highlighted that the deposition efficiencies derived from experiments obtained after iridium-192 inhalation were broadly consistent with the model prediction, although typically higher.

These inhalation campaigns will provide data in rats on the respiratory toxicological properties and toxicokinetics of inhaled nanoparticles of titanium dioxide and can be used to assess the capabilities of such materials to induce neuro-inflammation and to disrupt the blood-brain barrier.

This inhalation facility is not limited to the study of the toxicological properties of titanium dioxide nanoparticles; it can be readily adapted to other generators and other particle types, differing in terms of chemical nature, size, and concentration.

ACKNOWLEDGEMENT

The authors gratefully acknowledge Guillaume Antoine, Alexis Boivin, Stéphane Boucard, Mylène Lorcin, Mathieu Melczer, Lise Merlen, Jean-Claude Micillino, and Sylvie Sébillaud for their technical assistance. We also thank Marie-Joséphe Décret, Laurine Douteau, Lionel Dussoul and Sylvie Michaux from the laboratory animal facility for their help in rat handling and husbandry, and Vincent Jeandidier for drawing and design of the packed-tower humidifier, restraining tube and sampling adaptor.

REFERENCES

- Bau, S. and Witschger, O. (2013). A modular tool for analyzing cascade impactors data to improve exposure assessment to airborne nanomaterials. *J. Phys. Conf. Ser.* 429: 012002.
- Bermudez, E., Mangum, J.B., Wong, B.A., Asgharian, B., Hext, P.M., Warheit, D.B. and Everitt, J.I. (2004). Pulmonary responses of mice, rats, and hamsters to subchronic inhalation of ultrafine titanium dioxide Particles. *Toxicol. Sci.* 77: 347–357.
- Buckley, A., Hodgson, A., Warren, J., Guo, C. and Smith, R. (2016). Size-dependent deposition of inhaled nanoparticles in the rat respiratory tract using a new nose-only

- exposure system. *Aerosol Sci. Technol.* 50: 1–10.
- Charvet, A., Bau, S., Paez-Coy, N.E., Bémer, D. and Thomas, D. (2014). Characterizing the effective density and primary particle diameter of airborne nanoparticles produced by spark discharge using mobility and mass measurements (tandem DMA/APM). *J. Nanopart. Res.* 16: 2418.
- Charvet, A., Bau, S., Bémer, D. and Thomas, D. (2016). On the importance of density in ELPI data post-treatment. *Aerosol Sci. Technol.* 49: 1263–1270.
- Curwin, B. and Bertke, S. (2011). Exposure characterization of metal oxide nanoparticles in the workplace. *J. Occup. Environ. Hyg.* 8: 580–587.
- De Carlo, P.F., Slowik, J.G., Wornsop, D.R., Davidovits, P. and Jimenez, J.L. (2004). Particle morphology and density characterization by combined mobility and aerodynamic diameter measurements. Part 1: Theory. *Aerosol Sci. Technol.* 38: 1185–1205.
- Devoy, J., Brun, E., Cosnefroy, A., Disdier, C., Melczer, M., Antoine, G., Chalansonnet, M. and Mabondzo, A. (2016). Optimization of mineralization methods of TiO₂ nanoparticles: Determination of titanium levels in Rat organ tissues. *Toxicol. Lett.* 238: S202.
- Disdier, C., Devoy, J., Cosnefroy, A., Chalansonnet, M., Herlin-Boime, N., Brun, E., Lund, A. and Mabondzo, A. (2015). Tissue biodistribution of intravenously administered titanium dioxide nanoparticles revealed blood-brain barrier clearance and brain inflammation in rat. *Part. Fibre Toxicol.* 12: 27.
- Dong, Y., Hays, M.D., Smith, N.D. and Kinsey, J.S. (2004). Inverting cascade impactor data for size-resolved characterization of fine particulate source emissions. *J. Aerosol Sci.* 35: 1497–1512.
- Hsieh, T.H., Yu, C.P. and Oberdorster, G. (1999). A dosimetry model of nickel compounds in the rat lung. *Inhalation Toxicol.* 11: 229–248.
- Ma-Hock, L., Burkhardt, S., Strauss, V., Gamer, A., Wiench, K., van Ravenzwaay, B. and Landsiedel, R. (2009). Development of a short-term inhalation test in the rat using nano-titanium dioxide as a model substance. *Inhalation Toxicol.* 21: 102–118.
- Maricq, M.M., Xu, N. and Chase, R.E. (2006). Measuring particulate mass emissions with the electrical low pressure impactor. *Aerosol Sci. Technol.* 40: 68–79.
- Marjamäki, M., Lemmetty, M. and Keskinen, J. (2005). ELPI response and data reduction. I: Response functions. *Aerosol Sci. Technol.* 39: 575–582.
- Markowski, G.R. (1987). Improving Twomey's algorithm for inversion of aerosol measurement data. *Aerosol Sci. Technol.* 7: 127–141.
- Mauderly, J.L. (1982). The effect of age on respiratory function of Fischer-344 rats. *Exp. Aging Res.* 8: 31–36.
- McKinney, W., Chen, B. and Frazer, D. (2009). Computer controlled multi-walled carbon nanotube inhalation exposure system. *Inhalation Toxicol.* 21: 1053–1061.
- MDDE (2014). Éléments Issus Des Déclarations Des Substances À L'état Nanoparticulaires - Rapport D'étude 2014. 135 p (in French).
- Menache, M.G., Hanna, L.M., Gross, E.A., Lou, S.R., Zinreich, S.J., Leopold, D.A., Jarabek, A.M. and Miller, F.J. (1997). Upper respiratory tract surface areas and volumes of laboratory animals and humans: considerations for dosimetry models. *J. Toxicol. Environ. Health* 50: 475–506.
- Misra, C., Singh, M., Shen, S., Sioutas, C. and Hall, P.M. (2002). Development and evaluation of a personal cascade impactor sampler (PCIS). *J. Aerosol Sci.* 33: 1027–1047.
- Mitchell, L.A., Gao, J., Wal, R.V., Gigliotti, A., Burchiel, S.W. and McDonald, J.D. (2007). Pulmonary and systemic immune response to inhaled multiwalled carbon nanotubes. *Toxicol. Sci.* 100: 203–214.
- Morimoto, Y., Horie, M., Kobayashi, N., Shinohara, N. and Shimada, M. (2013). Inhalation toxicity assessment of carbon-based nanoparticles. *Acc. Chem. Res.* 46: 770–781.
- Noel, A., Cloutier, Y., Wilkinson, K.J., Dion, C., Halle, S., Maghni, K., Tardif, R. and Truchon, G. (2013). Generating nano-aerosols from TiQ₂ (5 nm) nanoparticles showing different agglomeration states. Application to toxicological studies. *J. Occup. Environ. Hyg.* 10: 86–96.
- Nurkiewicz, T.R., Porter, D.W., Hubbs, A.F., Cumpston, J.L., Chen, B.T., Frazer, D.G. and Castranova, V. (2008). Nanoparticle inhalation augments particle-dependent systemic microvascular dysfunction. *Part. Fibre Toxicol.* 5: 1.
- OECD (2009). Subacute Inhalation Toxicity: 28-Day Study. OECD Guideline for the Testing of Chemical 412.
- OECD (2015). Dossier on Titanium Dioxide - Part 1/3 - NM105, [http://www.oecd.org/officialdocuments/publicdisplaydocumentpdf/?cote=ENV/JM/MONO\(2015\)17/PAR/T1/3&docLanguage=En](http://www.oecd.org/officialdocuments/publicdisplaydocumentpdf/?cote=ENV/JM/MONO(2015)17/PAR/T1/3&docLanguage=En), p. 131.
- Ohtani, B., Prieto-Mahaney, O.O., Li, D. and Abe, R. (2010). What is Degussa (Evonik) P25? Crystalline composition analysis, reconstruction from isolated pure particles and photocatalytic activity test. *J. Photochem. Photobiol., A* 216: 179–182.
- Pauluhn, J. (2010). Subchronic 13-week inhalation exposure of rats to multiwalled carbon nanotubes: Toxic effects are determined by density of agglomerate structures, not fibrillar structures. *Toxicol. Sci.* 113: 226–242.
- R'Mili, B., Le Bihan, O.L.C., Dutouquet, C., Aguerre-Charriol, O. and Frejafon, E. (2013). Particle sampling by tem grid filtration. *Aerosol Sci. Technol.* 47: 767–775.
- Simon, X., Bau, S., Bémer, D. and Duquenne, P. (2015). Measurement of electrical charges carried by airborne bacteria laboratory-generated using a single-pass bubbling aerosolizer. *Particuology* 18: 179–185.
- Tiwari, A.J., Fields, C.G. and Marr, L.C. (2013). A cost-effective method of aerosolizing dry powdered nanoparticles. *Aerosol Sci. Technol.* 47: 1267–1275.
- Twomey, S. (1975). Comparison of constrained linear inversion and an iterative nonlinear algorithm applied to the indirect estimation of particle size distributions. *J. Comput. Phys.* 18: 188–200.
- Virtanen, A., Ristimäki, J. and Keskinen, J. (2004). Method for measuring effective density and fractal dimension of

- aerosol agglomerates. *Aerosol Sci. Technol.* 38: 437–446.
- Winklmayr, W., Wang, H.C. and John, W. (1990). Adaptation of the twomey algorithm to the inversion of cascade impactor data. *Aerosol Sci. Technol.* 13: 322–331.
- Yang, Y., Mao, P., Wang, Z.P. and Zhang, J.H. (2012). Distribution of nanoparticle number concentrations at a nano-TiO₂ plant. *Aerosol Air Qual. Res.* 12: 934–940.
- Zervas, E., Dorlhène, P., Forti, L., Perrin, C., Momiue, C., Monier, R., Ing, H. and Lopez, B. (2006). Exhaust gas particle mass estimation using an electrical low pressure impactor. *Energy Fuels* 20: 498–503.

Received for review, January 21, 2016

Revised, April 11, 2016

Accepted, April 22, 2016